

Understanding the Material Science of Battery We Use Everyday

Subir Paul*

Department of Metallurgical and Material Engineering, Jadavpur University, Kolkata, India

*Corresponding author: Subir Paul, Department of Metallurgical and Material Engineering, Jadavpur University, Kolkata, India, Fax: 913324572185; E-mail: spaul@metal.jdvu.ac.in

Received: April 07, 2017; Accepted: June 09, 2017; Published: June 16, 2017

Abstract

Development of existing and new batteries is a research thrust to meet the challenge of the global increasing demand of storage energy at lower price. The route to this development is through a better understanding of materials and electrochemistry of the existing batteries, so that new high energetic electrode materials are developed to enhance the performance of the batteries in use and to innovate new classes of energy storage systems. The present papers discuss the fundamental electrochemistry of battery design, working principles and materials of existing primary and rechargeable batteries with emphasis on new nano materials electrodes

Keywords: Anode; Cathode; Cell potential; Polarization; Nano synthesized electrodes; Electrochemical

1. Introduction

A battery is a form of storing electrical energy, produced by chemical energy conversion through the electrochemical reactions at anode and cathode. Theoretically the half-cell potentials of the anodic and cathodic reactions decide the open circuit cell potential of the battery. So the right choice of the two half-cell potentials from the TABLE 1 is the first step to design a battery. The cell potential can be obtained from the equation.

$$E^{\circ}_{\text{Cell}} = E^{\circ}_{\text{Red,Cathode}} + E^{\circ}_{\text{Red,Anode}} \quad (1)$$

For example, if a battery is made with:



One can write the half-cell reactions from the TABLE 1, such that on additions, electrons are nullified, as given below:

Cathode: $\text{PbO}_2(\text{s}) + 4\text{H}^+(\text{aq}) + 2\text{e}^- \rightarrow \text{Pb}_2^+(\text{aq}) + 4\text{H}_2\text{O}(\text{l})$ $E = +1.455$ volt

Anode: $\text{Pb} \rightarrow \text{Pb}_2^+(\text{aq}) + 2\text{e}^-$ $E = +0.125$ volt

Overall reaction: $\text{PbO}_2(\text{s}) + \text{Pb} + 4\text{H}^+(\text{aq}) = 2 \text{Pb}_2^+(\text{aq}) + 4\text{H}_2\text{O}$ $E = +1.85$ volt

If the half-cell potential is not available in the literature, the expected cell potential can be derived from the following equation. The free energy ΔG , of the overall reaction is related to cell potential E , by the equation.

$$\Delta G = -nFE \quad (2)$$

Where n is the no. of electron involved in each half cell reaction and F is the Faraday 96500 coulombs. For example if cell of Mg cathode and Cl_2 anode can be formed, the cell potential obtained would have been as follows:

$$E = (591.8 \times 1000) / (2 \times 96500) = 3.06 \text{ volt } (\Delta G \text{ for } \text{MgCl}_2 \text{ formation is } -591.8 \text{ kJ/m, (TABLE 2).}$$

TABLE 1. Standard electrode (reduction) potentials.

Reduction Half-Reaction, Acidic Solution	E° , V
$\text{F}_2(\text{g}) + 2\text{e}^- \rightarrow 2\text{F}^-(\text{aq})$	2.866
$\text{O}_3(\text{g}) + 2\text{H}^+(\text{aq}) + 2\text{e}^- \rightarrow \text{O}_2(\text{g}) + \text{H}_2\text{O}(\text{l})$	2.075
$\text{S}_2\text{O}_8^{2-}(\text{aq}) + 2\text{e}^- \rightarrow 2\text{SO}_4^{2-}(\text{aq})$	2.01
$\text{H}_2\text{O}_2(\text{aq}) + 2\text{H}^+(\text{aq}) + 2\text{e}^- \rightarrow 2\text{H}_2\text{O}(\text{l})$	1.763
$\text{MnO}_4^-(\text{aq}) + 8\text{H}^+(\text{aq}) + 5\text{e}^- \rightarrow \text{Mn}^{2+}(\text{aq}) + 4\text{H}_2\text{O}(\text{l})$	1.51
$\text{PbO}_2(\text{s}) + 4\text{H}^+(\text{aq}) + 2\text{e}^- \rightarrow \text{Pb}^{2+}(\text{aq}) + 4\text{H}_2\text{O}(\text{l})$	1.455
$\text{Cl}_2(\text{g}) + 2\text{e}^- \rightarrow 2\text{Cl}^-(\text{aq})$	1.358
$\text{Cr}_2\text{O}_7^{2-}(\text{aq}) + 14\text{H}^+(\text{aq}) + 6\text{e}^- \rightarrow 2\text{Cr}^{3+}(\text{aq}) + 7\text{H}_2\text{O}(\text{l})$	1.33
$\text{MnO}_2(\text{s}) + 4\text{H}^+(\text{aq}) + 2\text{e}^- \rightarrow \text{Mn}^{2+}(\text{aq}) + 2\text{H}_2\text{O}(\text{l})$	1.23
$\text{O}_2(\text{g}) + 4\text{H}^+(\text{aq}) + 4\text{e}^- \rightarrow 2\text{H}_2\text{O}(\text{l})$	1.229
$2\text{IO}_3^-(\text{aq}) + 12\text{H}^+(\text{aq}) + 10\text{e}^- \rightarrow \text{I}_2(\text{s}) + 6\text{H}_2\text{O}(\text{l})$	1.2
$\text{Br}_2(\text{l}) + 2\text{e}^- \rightarrow 2\text{Br}^-(\text{aq})$	1.065

$\text{NO}_3^-(\text{aq}) + 4\text{H}^+(\text{aq}) + 3\text{e}^- \rightarrow \text{NO}(\text{g}) + 2 \text{H}_2\text{O}(\text{l})$	0.956
$\text{Ag}^+(\text{aq}) + \text{e}^- \rightarrow \text{Ag}(\text{s})$	0.8
$\text{Fe}_3^+(\text{aq}) + \text{e}^- \rightarrow \text{Fe}_2^+(\text{aq})$	0.771
$\text{O}_2(\text{g}) + 2\text{H}^+(\text{aq}) + 2\text{e}^- \rightarrow \text{H}_2\text{O}_2(\text{aq})$	0.695
$\text{I}_2(\text{s}) + 2\text{e}^- \rightarrow 2\text{I}^-(\text{aq})$	0.535
$\text{Cu}_2^+(\text{aq}) + 2\text{e}^- \rightarrow \text{Cu}(\text{s})$	0.34
$\text{SO}_4^{2-}(\text{aq}) + 4\text{H}^+(\text{aq}) + 2\text{e}^- \rightarrow 2\text{H}_2\text{O}(\text{l}) + \text{SO}_2(\text{g})$	0.17
$\text{Sn}_4^+(\text{aq}) + 2\text{e}^- \rightarrow \text{Sn}_2^+(\text{aq})$	0.154
$\text{S}(\text{s}) + 2\text{H}^+(\text{aq}) + 2\text{e}^- \rightarrow \text{H}_2\text{S}(\text{g})$	0.14
$2\text{H}^+(\text{aq}) + 2\text{e}^- \rightarrow \text{H}_2(\text{g})$	0
$\text{Pb}_2^+(\text{aq}) + 2\text{e}^- \rightarrow \text{Pb}$	-0.125

TABLE 2. Free energy of formation of few compounds.

Species	Phase (Matter)
Aluminum Chloride	Solid
Magnesium Chloride	Solid
Manganese (IV) Oxide	Solid
Silica	Solid
Sodium Fluoride	Solid

Similarly, such high potential battery can be made with Si or other reactive metal but one needs to develop electrochemical science and technology for such battery. But the design of the cell needs to be such that the reaction is electrochemical not chemical; that is anodic and cathodic reactions are separated by a separator such as a membrane so that the electron released from the oxidation at anode is transported through the external load to the cathode which takes up this electron to complete the reduction reaction at cathode. The current delivered by the battery depends on many factors: electrochemical properties of electrocatalytic energy materials- anode and cathode; electrode surface area and conductivity of the electrolyte.

2. Fundamental of Electrochemistry in Battery

A battery consists of one or more electrochemical cells in series. The performance of the cell depends on the following components and parameters.

1. Anode and Cathode.
2. Electrolyte and Solvent.
3. Separator.
4. Cell Potential.

5. Cell Current.
6. Energy.

2.1 Anode and cathode

A good anode material should have the electro catalytic property for fast electrochemical oxidation along with good electrical conductivity, low polarization resistance, chemical stability and anti-corrosion property. A cathode material on other hand should have capacity to capture and transfer electron rapidly with high redox potential besides low polarization resistance. The materials for anode and cathode in common batteries are shown in TABLE 3. But new high energetic electrocatalytic materials are being developed. Several oxides and metal alloys have been found to show good electro catalytic properties. Materials such as CoTi [1], PbO₂ [2], TiO₂ [3] and β-MnO₂ [4] show very encouraging results for application in fuel cell electrodes.

2.1.1 Nano materials electrodes: The superior electrocatalytic property at nanoscale is broadly due to the fact that nanomaterials have relatively larger surface area compared to the same mass of the material produced in larger form. Nanostructured materials provide additional electrode surface area with short path lengths for electronic and ionic transport and thus the possibility of higher reaction rates.

It has been found by authors and his group that nano-materials electrodes are very high energetic electro catalytic surface. Paul et al. [5-7], produced MnO₂ and MnO₂-nano carbon electrodes by electro synthesis to produce clean energy through a fuel cell, using glucose as fuel. Nano composite metal oxides, ZnO-Al₂O₃ produced by paul et al. [8] performed as very good electro catalytic energy material as glucose fuel cell electrode. There are a few works on Ni based alloy electrodes. Nano-coated Ni-based alloys have also been investigated by Paul et al. for inexpensive fuel cell electrode for energy applications [9,10].

It has been reported that the rare earth oxide CeO₂ with cation vacancy state between +3 and +4, is a source of oxygen on the electrode catalytic surface and therefore enhances the electrode reactions. Thus, addition of CeO₂ to the metal electrode has been reported to enhance the electro-oxidation property by several times [11-14].

2.2 Current collector

If the anode or cathode is not a single conduction solid plate/sheet but granule or powder metal oxide or compounds, then a current collector is placed into the granule electrode materials to receive or deliver electron from the anode or cathode respectively. An anode collector, the negative terminal, which accepts electron released by the anodic oxidation at anode-electrolyte interface. A cathode collector, the positive terminal, which accepts electron from the anodic through the external load and passes to cathode for discharge reaction at cathode-electrolyte interface.

2.3 Electrolyte and solvent

An electrolyte is an ionic aqueous or non-aqueous compound, with a common anions or cations associated with the anions or cations of the electrode reaction. It must have good ionic conductivity and be able to easily dissociate into its ions. A solvent

is also another ionic compound where electrolyte can be dissolved. It is of high ionic conductivity. In alkaline aqueous environment KOH solution is a good solvent for many batteries and fuel cells. Non-aqueous solvent such as organic liquids are required under the conditions when water may be electrolytically decomposed into hydrogen and oxygen.

2.4 Separator

These electrodes must be separated by and are often immersed in an electrolyte that permits the passage of ions between the electrodes. The electrode materials and the electrolyte are chosen and arranged so that sufficient electromotive force (measured in volts) and electric current (measured in amperes) can be developed between the terminals of a battery to operate lights, machines, or other devices. Since an electrode contains only a limited number of units of chemical energy convertible to electrical energy, it follows that a battery of a given size has only a certain capacity to operate devices and will eventually become exhausted. The active parts of a battery are usually encased in a box with a cover system (or jacket) that keeps air outside and the electrolyte solvent inside and that provides a structure for the assembly.

A separator is needed for liquid electrolyte. The separator film is soaked in the electrolyte and held in place. A separator should have high electrolyte permeability and low air permeability to have low cell resistivity; suitable porosity (about 40%) pore size small enough to prevent anode/cathode products; good wettability by the electrolyte for absorption and retention; good chemical, thermal and dimensional stability; high puncture and tensile strength. It should be an electronic insulator, having minimum electrolyte resistance in high electrochemical active environment. They are either made into sheets and assembled with the electrodes or deposited onto the electrode *in situ*.

Examples: Polyethylene, polypropylene.

2.5 Cell potential, E-cell

The anodic reaction at anode-electrolyte interface is an electrochemical oxidation with a half cell potential under standard state is E_a^0 . The cathodic reaction at cathode-electrolyte interface is a reduction reaction with a standard half-cell potential E_c^0 .

The open circuit standard cell potential of the battery is given as:

$$E_{\text{cell}}^0 = E_c^0 - E_a^0 \quad (3)$$

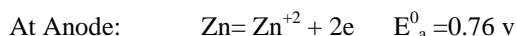
But if the reactants and products are not at standard conditions, the cell potential is found by Nernst equation as follows.

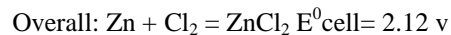
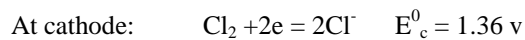
For an overall reaction, consisting of two half-cell reactions of anode and cathode is given as:

$$aA + bB = cC + dD$$

$$E_{\text{cell}} = E_{\text{cell}}^0 - \frac{RT}{nF} \ln \left(\frac{(aC)^c (aD)^d}{(aA)^a (aB)^b} \right) \quad (4)$$

Let us take an example of Zn/ Cl₂ battery:





$$E_{\text{cell}} = E_{\text{cell}}^0 - (RT/2F) \ln\left(\frac{[\text{ZnCl}_2]}{[\text{Zn}^{+2}] (\text{Cl}_2)}\right)$$

If the pressure of Cl_2 is 1 atm and ZnCl_2 is pure substance, Zn^{+2} at 1 molar concentration at $T=298 \text{ K}$ RT/F 0.059 volts.

$$E_{\text{cell}} = 2.12 - 0.0285 \ln(1/0.1) \quad (5)$$

The equation (2) and (3) give open circuit potential of the cell. Using the TABLE 1, one can find the other combinations of anode and cathode.

2.6 Onload potential

The cell potential obtained by equation (2) decreases, the moment the +ve and -ve terminals are connected through an external load due to polarizations of the electrode, the magnitude represented by overvoltage η and internal resistance of the cell.

The net cell potential is given by the equation (6).

$$E_{\text{cell, net}} = E_{\text{cell}} - \eta - IR \quad (6)$$

Where η is total over voltage at anode and cathode, R is the electrolyte resistivity, I current passing through the cell.

The overvoltage has two parts activation Polarization η_{act} and Concentration Polarization η_{con}

So that,

$$\eta = \eta_{\text{act}} + \eta_{\text{con}} \quad (7)$$

2.6.1 Overvoltage due to activation polarization η_{act} : It is given by Tafel's equation as follows:

$$\eta_{\text{act}} = \pm \beta \log(i/i_0) \quad (8)$$

where β is the Tafel's slope, i_0 is the exchange current density.

For anodic reaction

$$\eta_{\text{act, a}} = + \beta_a \log(i_a/i_0) \quad (8.1)$$

2.6.2 Overvoltage due to concentration polarization η_{con}

For Cathodic reaction

$$\eta_s = - \beta_c \log(i_c/i_0) \quad (8.2)$$

The concentration of the reducing species in the electrolyte near the cathode varies with a stagnant diffusion barrier, known as Nernst diffusion layer. Concentration of M^{++} ions decreases from the bulk solution towards the metal-solution interface. The speed at which electron is transported at the cathode is much greater than the speed of diffusion of ions towards the

electrode surface. The concentration polarization arises due to non-availability of the ions, to be reduced by waiting electrons at the cathode. When the concentration of the ion at the electrode surface becomes zero, it is the limiting case and polarization approaches negative infinity (FIG. 1). The current corresponding to this situation is the limiting current density i_L [9,10].

$$\eta_{con} = 2.33RT/(nF) \log (1- i/i_L) \tag{9}$$

$$\eta_{con,a}=2.33RT/(nF) \log (1- i_a/i_L) \tag{9.1}$$

$$\eta_{con,c}=2.33RT/(nF) \log (1- i_c/i_L) \tag{9.2}$$

$$i_L = DnFC_B/d \tag{10}$$

So the net cell potential is given by the equation (11) and is also schematically shown in FIG.1.

$$E_{cell,net} = E_{cell} - \eta_{act,a} - \eta_{act,c} - \eta_{con,a} - \eta_{con,c} - IR \tag{11}$$

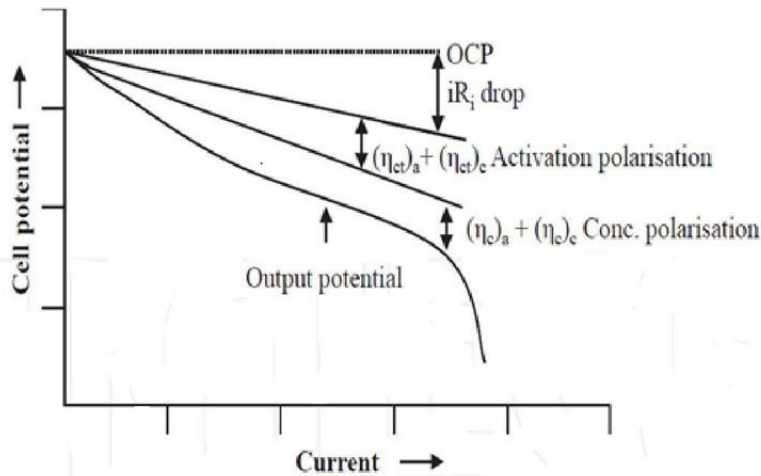


FIG. 1. Schematic diagram showing the different polarization effects on battery cell potential.

So to get high cell potential and hence energy, all the overvoltage terms in the equation above by developing high electrocatalytic electrode materials, anode and cathode, low electrolyte resistance R .

The current (I) is given as,

$$I = E_{cell,net}/R_L \tag{12}$$

Where R_L is the external load

$$G=Energy = IE_{cell,net} \times h = \text{Ampere} \times \text{voltage} \times \text{hour} = \text{watt-hour} \tag{13}$$

Electrode material consumption and specific energy

So specific energy,

$$G_{sp} = (IE_{cell,net} \times h) / M \tag{14}$$

Where M is the aggregate mass of anode consumption and product generation at cathode.

3. Primary and Secondary Batteries

Batteries are divided into two general groups: (1) primary batteries and (2) secondary, or rechargeable batteries. Primary batteries are designed to be used until the voltage is too low to operate a given device and are then discarded. Secondary batteries have many special design features, as well as particular materials for the electrodes, that permit them to be reconstituted (recharged).

After partial or complete discharge, they can be recharged by the application of direct current (DC) voltage. While the original state is usually not restored completely, the loss per recharging cycle in commercial batteries is only a small fraction of 1 percent even under varied conditions.

Battery usefulness is limited not only by capacity but also by how fast current can be drawn from it. The salt ions chosen for the electrolyte solution must be able to move fast enough through the solvent to carry chemical matter between the electrodes equal to the rate of electrical demand. Battery performance is thus limited by the diffusion rates of internal chemicals as well as by capacity.

3.1 Zinc carbon battery

FIG. 2, schematically shows the detail of materials of construction of the battery.

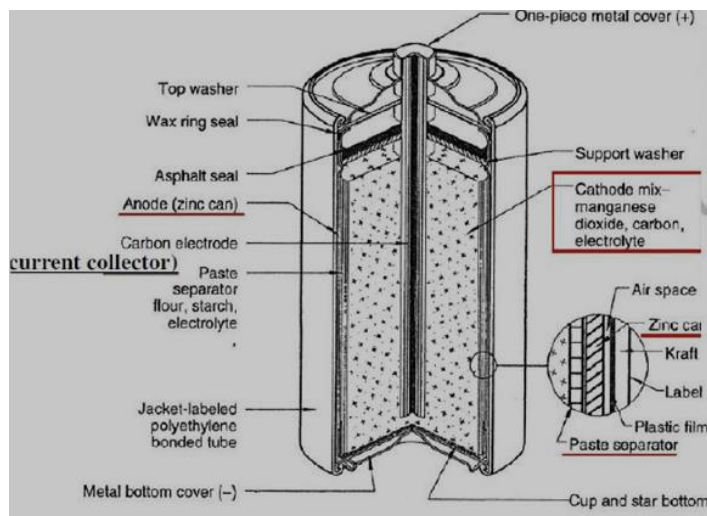


FIG. 2. Schematic diagram showing materials and inner construction of Zn-Carbon battery.

Anode: Zn + 0.2-0.4% Pb (corrosion inhibitor + forming) + 0.03% - 0.06% Cd (corrosion resistance + strength)

Cathode: MnO₂ (poor electrical conductivity) + Carbon black (for electrical conductivity and retain moisture)

Electrolytes:

1. 26.0% NH₄Cl + 8.8% ZnCl₂ + 65.2% H₂O (low pH) + 0.25% - 1% Zn corrosion inhibitor
2. 15% - 40% ZnCl₂ + 85% - 60% H₂O + 0.02% - 1% Zn corrosion inhibitor.

The corrosion inhibitor in the electrolyte may be Hg + HgCl₂ (bad for environment) or Ga, In, Bi, Sn. The inhibitor is used to prevent Zn to corrode to ZnCl₂.

Cathode current collector: Carbon rod.

Anode current collector: Zn can.

Separator: Starch paste.

Paper reactions:

Anodic: Zn = Zn⁺⁺ + 2e

Cathodic: 2MnO₂+2e = Mn₂O₃+ O⁻²

Overall reaction: Zn + 2MnO₂ = ZnO + Mn₂O₃ E_{cell} = 1.5 volt - 1.6 volt

3.2 Alkaline MnO₂ Battery

The construction of the battery has been shown in FIG. 3.

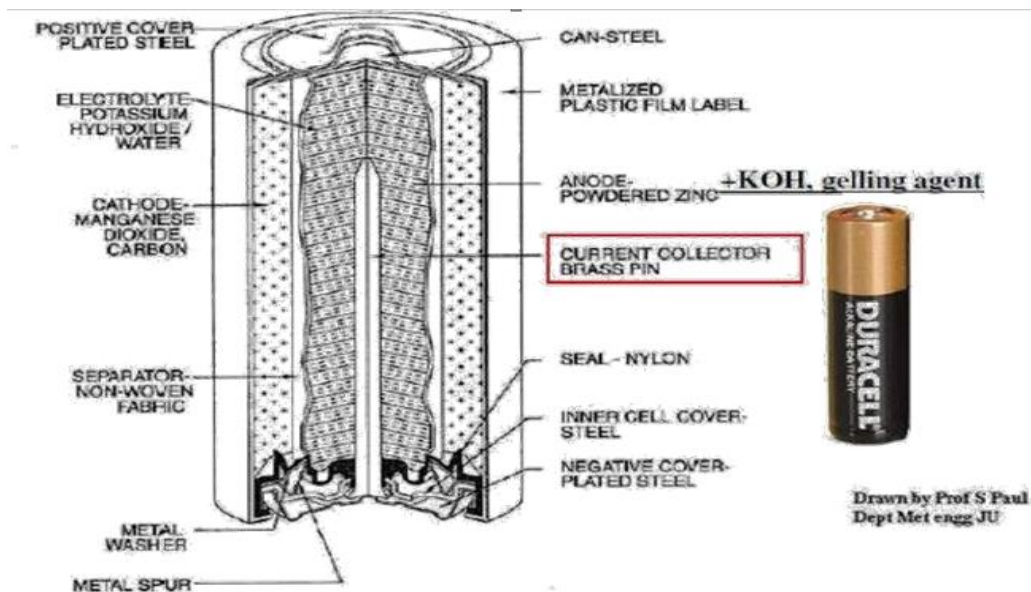


FIG. 3. Schematic diagram showing materials and inner construction of Alkaline MnO₂ battery.

Anode: Zn powder, high surface area.

Cathode: 70% - 90% high activity Electrolytic MnO₂ (EMD) + 2% - 10% Carbon (Electronic Conductor) + 0% - 1% binding agent (optional).

Electrolyte: 35% - 52% KOH aqueous solution.

EMD is produced by electrolytic decomposition as follows:



Reactions:

Anode: $\text{Zn} + 2\text{OH}^- = \text{Zn}(\text{OH})_2 + 2\text{e}$

Cathode: $2\text{MnO}_2 + 2\text{e} + \text{H}_2\text{O} = 2\text{MnOOH} + 2\text{OH}^-$

Overall reaction: $\text{Zn} + 2\text{MnO}_2 = \text{Zn}(\text{OH})_2 + 2\text{MnOOH}$

$E_{\text{cell}} = 1.5 \text{ V} - 1.6 \text{ V}$

3.3 Zinc - Silver oxide battery

FIG. 4, schematically shows the detail of materials of construction of the battery.

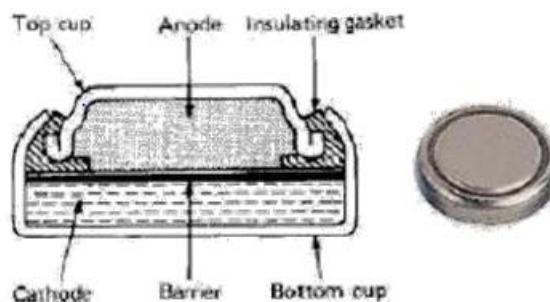


FIG. 4. Schematic diagram showing materials and inner construction of Zn – Silver Oxide battery.

Anode: Zinc

Cathode: Silver Oxide

Electrolyte: potassium hydroxide

Reactions:

Anode: $\text{Zn} + 2\text{OH}^- = \text{Zn}(\text{OH})_2 + 2\text{e}$

Cathode: $\text{Ag}_2\text{O} + 2\text{e} + \text{H}_2\text{O} = 2\text{Ag} + 2\text{OH}^-$

Overall reaction: $\text{Zn} + \text{Ag}_2\text{O} + \text{H}_2\text{O} = 2\text{Ag} + \text{Zn}(\text{OH})_2$

$E_{\text{cell}} = 1.59 \text{ v}$

Zinc-Air battery

The construction of the battery is shown in FIG. 5.

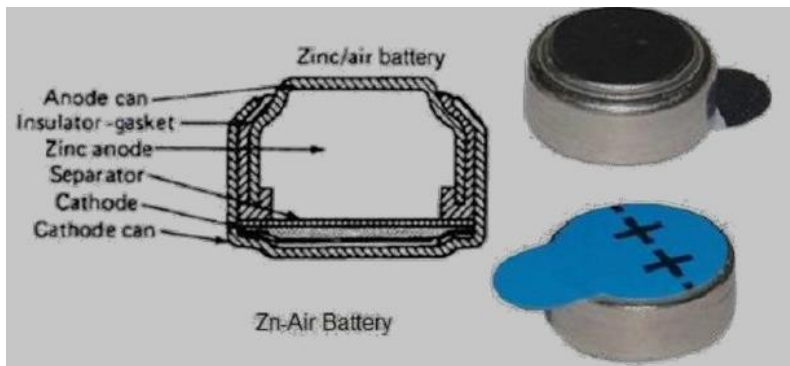


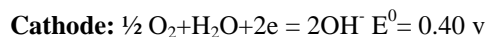
FIG. 5. Schematic diagram showing materials and inner construction of Zn – air battery.

Anode: Zn

Cathode: Electro Catalytic Metal Oxide or Noble metal

Electrolyte: KOH solution

Reactions:



Rechargeable Batteries

Lead –Acid battery

The construction of the battery is shown in FIG. 6.

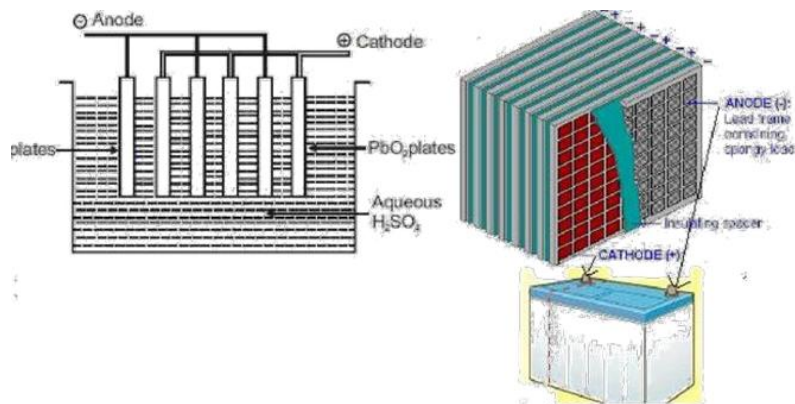


FIG. 6. Schematic diagram showing materials and inner construction of Lead - Acid battery.

Anode: Pure Lead in soft sponge condition.

Cathode: Lead peroxide. This is dark brown, hard and brittle substance

Electrolyte: Dilute sulfuric acid, ratio of water: acid = 3:1.

Reaction (discharge)

Anode: $\text{PbO}_2(\text{s}) + \text{HSO}_4^{-}(\text{aq}) + 3\text{H}^+(\text{aq}) + 2\text{e}^- \rightarrow \text{PbSO}_4(\text{s}) + 2\text{H}_2\text{O}(\text{l})$ $E^0 = 0.356 \text{ eV}$

Cathode: $\text{PbO}_2(\text{s}) + \text{HSO}_4^{-}(\text{aq}) + 3\text{H}^+(\text{aq}) + 2\text{e}^- \rightarrow \text{PbSO}_4(\text{s}) + 2\text{H}_2\text{O}(\text{l})$ $E^0 = 1.685$

Overall: $\text{Pb}(\text{s}) + \text{PbO}_2(\text{s}) + 2\text{H}_2\text{SO}_4(\text{aq}) \rightarrow 2\text{PbSO}_4(\text{s}) + 2\text{H}_2\text{O}(\text{l})$ $E_{\text{cell}} = 2.041 \text{ V}$ at 1 M acid conc, 298 K

Cathode: Lead peroxide (PbO_2) filled into Pb grids

Anode: Sponge lead (Pb)

Electrolyte: dil H_2SO_4 water: acid = 3:1

Discharging: H_2SO_4 dissociates $\text{H}_2\text{SO}_4 = \text{H}^+ + \text{HSO}_4^+$

At cathode (PbO_2)

$\text{PbO}_2(\text{s}) + 3\text{H}^+ + \text{HSO}_4^+ + 2\text{e}^- = \text{PbSO}_4(\text{s}) + 2\text{H}_2\text{O}$

At anode: Pb

$\text{Pb}(\text{s}) + \text{HSO}_4^+ = \text{PbSO}_4(\text{s}) + \text{H}^+ + 2\text{e}^-$

So, both cathode and anode plates become PbSO_4 during discharging.

Overall $\text{Pb} + \text{PbO}_2 + 2\text{H}_2\text{SO}_4 \rightarrow 2\text{PbSO}_4 + 2\text{H}_2\text{O}$

Charging: Using external dc supplies, the battery is charged. Of course, during recharge, the opposite redox reactions occur.

Hydrogen ions (cation) being positively charged, move to the electrode (cathode) connected with negative terminal of the DC source. Here each H^+ ion takes one electron from that and becomes hydrogen atom. These hydrogen atoms then attack PbSO_4 and form lead and sulfuric acid.

At cathode (previously anode during discharging):

$\text{PbSO}_4(\text{s}) + \text{H}^+ + 2\text{e}^- = \text{Pb}(\text{s}) + \text{HSO}_4^+$

At anode (previously cathode during discharging):

$\text{PbSO}_4(\text{s}) + 2\text{H}_2\text{O} = \text{PbO}_2(\text{s}) + 3\text{H}^+ + \text{HSO}_4^+ + 2\text{e}^-$

So, after charging PbSO_4 at anode and cathode are converted back to Pb and PbO_2 respectively.

During the discharge operation, acid is consumed and water is produced. During the charge operation, water is consumed and acid is produced because sulfuric acid is much denser than water, a widely-used technique for checking the state-of-charge of a battery is to measure the specific gravity of the electrolyte. One practical consequence is that you can measure how fully charged the battery is by measuring the density of the electrolyte using a hydrometer.

The lead sulfate (PbSO_4) is whitish in color.

During discharging,

1. Both of the plates are covered with PbSO_4 .
2. Specific gravity of sulfuric acid solution falls due to formation of water during reaction at PbO_2 plate.
3. As a result, the rate of reaction falls which implies the potential difference between the plates decreases during discharging process.

Hence by charging the lead acid storage battery cell,

1. Lead sulfate anode gets converted into lead peroxide.
2. Lead sulfate of cathode is converted to pure lead.
3. Terminal potential of the cell increases.
4. Specific gravity of sulfuric acid increases.

3.6 Ni-Cd battery

FIG. 7, schematically shows the detail of materials of construction of the battery.

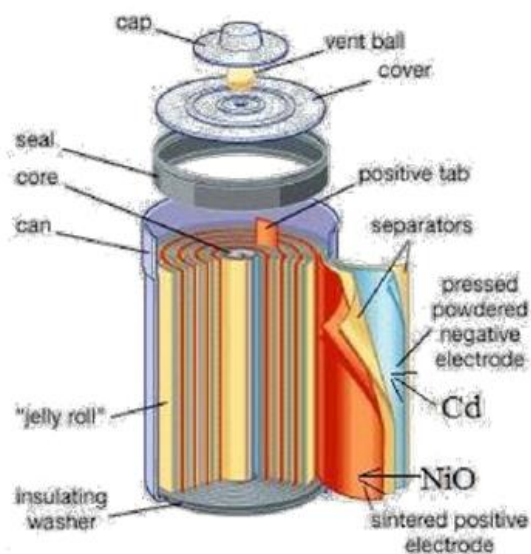


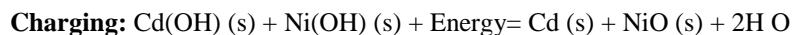
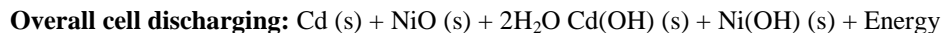
FIG. 7. Schematic diagram showing materials and inner construction of Ni-Cd battery.

Anode: Cadmium

Cathode: Nickel Oxide

Electrolyte: KOH

When the nickel battery operates, Cd is oxidized to Cd ions at anode and the insoluble Cd(OH) is formed. NiO is reduced to Ni ions which further combines with OH ions to form Ni(OH). It produces about 1.4 V.



3.7 Ni-MH Battery

Ni-Cd battery is replaced by higher performance Ni-MH battery. The construction of the battery is shown in FIG. 8.

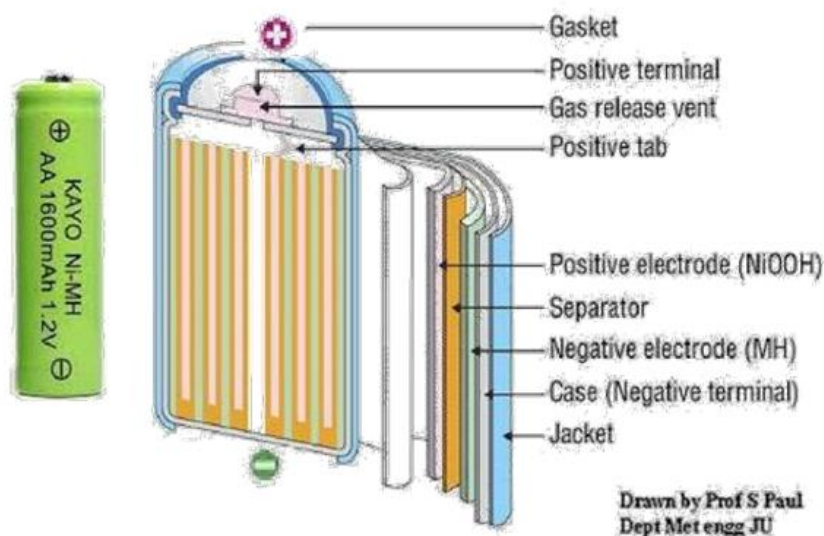


FIG. 8. Schematic diagram showing materials and inner construction of Ni-MH battery.

Anode: Metal hydride (consisting of V, Ti, Ni & other metals)

Cathode: Nickel Oxyhydroxide (NiOOH)

Electrolyte: KOH



Ni(OH)₂ has 2 polymorphic forms α- Ni(OH)₂ and β- Ni(OH)₂. On anode MH is dehydrogenated to M and H⁺ which is electrochemically oxidized to H₂O. The metal alloy is capable of reversible hydrogen adsorption/desorption as the battery is cycled. The metal hydride should have capacity to hydrogen adsorption/desorption as well as high corrosion resistance against oxidation in concentrated KOH solution.

3.8 Li ion battery

Li possesses very low electronegativity and denotes electron the easiest to form positive ion. The standard cell potential is 3.045 V. Its light weight with combination of high potential and energy density makes it superior rechargeable battery. However, Li has a serious problem of dendrite formation on its surface during charge/discharge. To avoid the problem, instead of using pure Li, it is intercalated between metal oxide strips as shown in the FIG. 9. The cathode is Li transition metal oxide such as LiCoO_2 , LiNiO_2 , or LiMn_2O_4 and anode is graphite.

Electrolyte: KOH

Anode: $\text{MH} + \text{OH}^- = \text{M} + \text{H}_2\text{O} + \text{e}^-$

Cathode: $\text{NiOOH} + \text{H}_2\text{O} + \text{e}^- = \text{Ni(OH)}_2 + \text{OH}^-$

Overall cell: $\text{NiOOH} + \text{MH} \text{ charge/discharge } \text{Ni(OH)}_2 + \text{M} \quad E_{\text{cell}} = 1.2 \text{ v}$

Ni(OH)_2 has 2 polymorphic forms α - Ni(OH)_2 and β - Ni(OH)_2 . On anode MH is dehydrogenated to M and H^+ which is electrochemically oxidized to H_2O . The metal alloy is capable of reversible hydrogen adsorption/desorption as the battery is cycled. The metal hydride should have capacity to hydrogen adsorption/desorption as well as high corrosion resistance against oxidation in concentrated KOH solution.

3.8 Li ion battery

Li possesses very low electronegativity and denotes electron the easiest to form positive ion. The standard cell potential is 3.045 V. Its light weight with combination of high potential and energy density makes it superior rechargeable battery. However, Li has a serious problem of dendrite formation on its surface during charge/discharge. To avoid the problem, instead of using pure Li, it is intercalated between metal oxide strips as shown in the FIG. 9. The cathode is Li transition metal oxide such as LiCoO_2 , LiNiO_2 , or LiMn_2O_4 and anode is graphite.

Anode: Graphite

Cathode: LiCoO_2 or LiNiO_2 , or LiMn_2O_4

Electrolyte: 1M LiPF_6 dissolved in a mixture of organic solvents, ethylene carbonate and dimethyl carbonate (1:1 by volume).

Anodic reaction: $x\text{Li} (\text{graphite}) = x\text{Li}^+ + \text{xe}^-$

Cathodic reaction: $x\text{Li}^+ + \text{xe}^- + \text{LiCoO}_2 = \text{Li}_{1+x}\text{CoO}_2$ or $x\text{Co}_4^+ + \text{xe}^- = x\text{Co}_3^+$

Discharge/charge

Overall cell: $x\text{Li} + \text{LiCoO}_2 \leftrightarrow \text{Li}_{1+x}\text{CoO}_2 \quad E_{\text{cell}} = 3.0 \text{ v}$

4. Performance of Existing Batteries

The performance of a battery is decided by good cell potential 1.5-3.5 volt, high delivering current and hence high specific energy (Ah/kg or Ah/l), good no of cycles of charge-discharge with minimum energy drainage. The performance of the different batteries is schematically shown in FIG. 10.

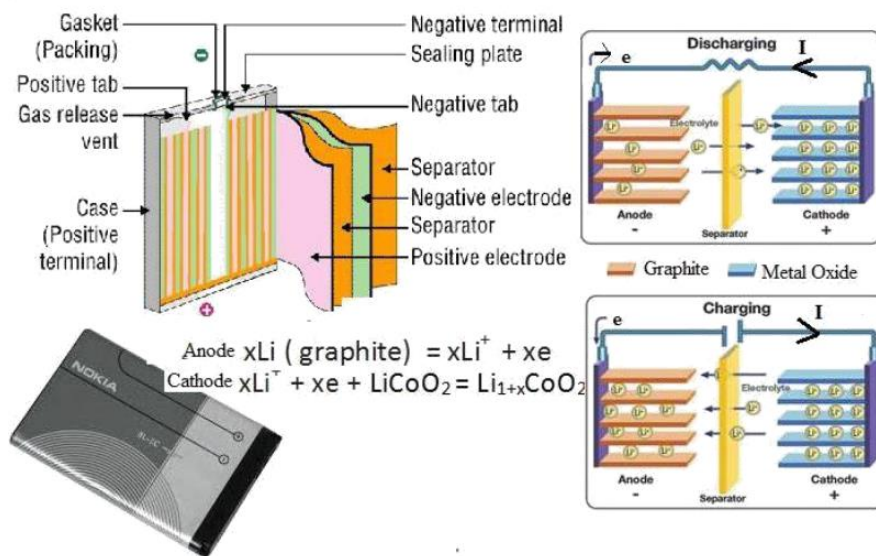


FIG. 9. Schematic diagram showing materials and inner construction of Ni-MH battery.

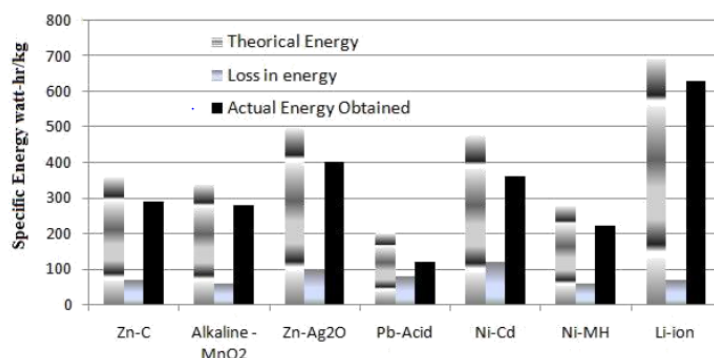


FIG. 10. Comparison of specific energy of different primary and rechargeable cell.

It is seen for all the batteries the actual specific energy obtained is much less than theoretical specific energy. The loss in energy is due to one or more of following effects:

1. Anode and cathode over voltage for anodic and cathodic reactions that is polarization.
2. High hydrogen overvoltage at cathode.
3. High oxygen overvoltage at anode.
4. High IR drop that is high electrolyte conductivity.
5. Restricted reversible reactions at anode and cathode electrodes to maintain specific charge for hundreds of charge and discharge cycles.

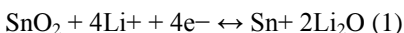
To minimize the energy losses, newer high energetic electrode materials need to be developed. There are a large number of elements and compounds from which to select potentially useful combinations for batteries. Nanostructured materials provide additional electrode surface area with short path lengths for electronic and ionic transport and thus the possibility of higher

reaction rates. It has been found by authors and his group that nano materials electrodes are very high energetic electro catalytic surface [6-10]. The authors Paul, Jana and Mondal [11-18] have achieved to synthesize clean electrical energy from different biofuels, using these high energetic nanomaterial electrodes in fuel cells.

Besides the above factors there are economic factors to be considered for commercialization, low cost electrode materials & manufacturing process, inexpensive electrolyte, operation at room temperature or little above room temperature, completely sealed & environment friendly.

4.1 Development of existing batteries

Research works to develop these electrodes materials can improve the performance of the batteries. The oxide materials in the existing battery can be replaced by nanostructure materials. Nanostructured materials provide additional electrode surface area with short path lengths for electronic and ionic transport and thus the possibility of higher reaction rates. It has been found by authors and his group [5-8] that MnO_2 nano carbon electrodes show excellent electrocatalytic properties and the cost is also not high. Researchers and engineers in battery industry may further work on it for alkaline MnO_2 and Zn-C batteries. Nano-coated Ni-Co alloys synthesized and investigated by the author exhibit excellent electrochemical property for battery energy applications [9,10]. The material exhibited low polarization resistance and high exchange current density, that enhanced the rate of charge-discharge reaction on the electrode surface. Battery makers can use this material in Ni-Cd battery. Nano composite metal oxides, $\text{ZnO-Al}_2\text{O}_3$ produced by Paul et al. [8] performed as very good electro catalytic energy electrode. Li ion battery is the most popular and commercially used in Laptop and mobile phones. There are new developments of cathode and anode materials for Li ion battery. They are illustrated in TABLES 3A and 3B respectively. Metal oxides have been studied intensively as anode materials for LIBs, such as Ti-based oxides (TiO_2 [19] and $\text{Li}_4\text{Ti}_5\text{O}$ [20]), Mn-based oxides (MnO [21], Mn_3O_4 [22], Mn_2O_3 [23] and MnO_2 [24]), Fe-based oxides (Fe_3O_4 [25] and Fe_2O_3 [26]), Co_3O_4 [27], NiO [28] and SnO_2 [29]. Among them, SnO_2 is believed to be the most promising candidate, because of its low cost, environmental benignity and high theoretical specific capacity [29,30]. More importantly, SnO_2 has the lowest operating voltages (average discharge and charge voltages of 0.3 V and 0.5 V vs. Li/Li^+ , respectively) compared to the other transition metal oxides so that the energy density of full cells would be higher when SnO_2 is used as anode material [29,31]. For SnO_2 based electrode, the electrochemical processes involve the following two steps [31,32]:



For bulk SnO_2 materials, the first reaction is believed to be irreversible so that the theoretical capacity is about 780 mAh g^{-1} [31,33,34]. While for nano-sized SnO_2 particles, it is reported that the first reaction becomes reversible/part reversible and the theoretical capacity can increase to the largest value of 1494 mAh g^{-1} [31,35], which is about three times higher than that of the commercialized graphite (only 372 mAh g^{-1}). The second process is widely known to be reversible and the lithium can be repeatedly alloyed and dealloyed with Sn formed in.

5. Future Batteries

To start with finding a new battery with high energy and cell potential, a combination of highly reactive metals with high electronegative anions is the first step. Most of the investigated, high-voltage ionic shuttles (Li, Na, and Mg) are located at the negative end of the standard electrode potential series. The other end of the standard potential series, which comprises materials such as fluorine and chlorine have not been deeply investigated for batteries. The list of future batteries are Fluoride ion battery, Chloride ion battery, Mg battery, Na battery, Al battery, Zn battery. TABLE 4, gives a comparison of specific energy of a few

TABLE 3A. Materials in common primary batteries.

Type	Anode	Cathode	Electrolyte
Zinc-Carbon (Leclanché)	Zinc Alloy	Manganese Dioxide Cathode	80 Percent Ammonium Chloride and 20 Percent Zinc Chloride
Zinc Chloride	Zinc	Manganese Dioxide	--
Zinc-Manganese Dioxide	Zinc	Manganese Dioxide	Potassium Hydroxide
Zinc-Silver Oxide	Zinc	Silver Oxide	Potassium Hydroxide
Zinc-Air	Zinc	Oxygen	Potassium Hydroxide
Lithium-Iron Sulfide	Lithium	Iron Sulfide	Organic Electrolyte;
Lithium- Manganese Dioxide	Lithium	Manganese Dioxide	Organic Electrolyte

TABLE 3B. Materials in rechargeable batteries.

Type	Anode	Cathode	Electrolyte
Lead-Acid	Lead	Lead Dioxide	Sulfuric Acid
Nickel-Cadmium	Cadmium	Nickel Dioxide	Potassium Hydroxide
Nickel-Metal Hydride	Lanthanide Or Nickel Alloy	Nickel Dioxide	Potassium Hydroxide Electrolyte
Lithium-Ion	Carbon	Lithium Cobalt Dioxide	Organic Electrolyte

batteries. Among these the development of the most promising future batteries are discussed. For the development of the electrode materials all testing in the sections 3.0 are to be followed.

5.1 Fluoride Ion Battery

Fluorine is the most electronegative element in the periodic table. Thus, the fluoride ion is very stable and has a wide electrochemical stability window. It can therefore be regarded as a suitable and stable ion for charge transfer in a battery. There are only a few works on fluoride ion battery [34-38].

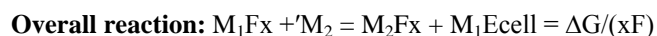
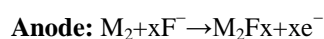
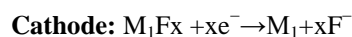
TABLE 4. Comparison of specific energy of future batteries.

Species	Energy capacity mAh/mL	Specific Energy mAh/g	Reduction Potential V vs. SHE	Effective ionic radius (Å)
Li	2026	3861	-3.04	0.76
Na	1128	1165	-2.71	1.02
K	591	685	-2.93	1.38
Mg	3833	2205	-2.37	0.72
Ca	2073	1337	-2.87	1
Zn	5851	820	-2.2	0.74
Al	8040	2980	-1.67	0.54

The transfer of the fluoride ion between two electrodes enables reversible storage of electrons by charge compensation when the electrochemical couple is either charged or discharged by the outer electric circuit of the battery. The theoretical working principle of a FIB is illustrated with an example of BiF₃/Mg as electrochemical couple. The discharge is accompanied by the oxidation of the anode, e.g., Mg → MgF₂, which releases two electrons to the electric circuit.

The electrons reduce the cathode (consisting of a metal fluoride) to the corresponding metal, such as in BiF₃ → Bi. Charge neutrality is assured by F⁻. In theory, there is no fundamental property that renders fluoride ion batteries (FIBs) inherently more dangerous than other state-of-the-art batteries as long as appropriate safety measures are applied. But it has to be said, that such design principles remain to be established and therefore no clear statement on the safety is possible at the moment.

For binary fluorides, these reactions are of the following types:



where M1 is the metal used in the cathode, M2 is the metal used in the anode, and m or n is the number of fluoride ions.

The battery was operated at 150°C by using a solid electrolyte of a LaF₃/BaF₂ composite with a fluoride conductivity of 0.2 mS cm⁻¹ at ~150°C.

5.2 Chloride ion battery

Metal chloride/metal systems show a large Gibbs free energy change yielding a high electromotive force (EMF) during the phase transformation, i.e., the chloride ion transfer. The data of energy densities for some electrochemical couples of these systems are listed in TABLE 4. The metal chloride/metal systems show theoretical energy densities which are above those of the current LIB. Moreover, this battery system can be built from abundant material resources and it is possible to use various metals (e.g. Li, Na, Mg, Ca, and Ce) or their chlorides as active material in the electrode. Thus, it is interesting to explore these systems based on chloride ion transfer in the field of rechargeable batteries, which has not been reported so far. A key challenge is the development of electrolytes with high chloride ion conductivity.

Solid inorganic compounds such as PbCl₂, SnCl₂, and LaOCl show fast chloride transfer at very high temperatures [39] and [40], which are even higher than the melting points of some metal chlorides. The cubic CsSnCl₃ has a high ionic conductivity of 1 mS cm⁻¹ at about 100°C as studied by Stevens [41] and Wang [42], but its electrochemical stability needs to be investigated.

5.3 Mg Battery

Mg as anode material has the potential advantage of a high theoretical volumetric capacity of 3832 mAh/cm³ (Li: 2062 mAh/cm³), its electrochemical potential is -2.37 V vs. NHE. Interestingly, Mg does not form dendrites when electrodeposited and can therefore be used in metallic form, thus avoiding inert host materials like in the Li/graphite system. Mg is environmentally benign, safe to handle and of low cost compared to lithium. With proper design and architecture could also lead to gravimetric energy densities of ~150–200 W h/kg with an operating voltage in the ~2–3 V range making it an attractive candidate for electrical storage systems supporting wind and solar energy, distributed energy systems, or grid operation. Sulfur or its composite can be used as cathode. The electrochemical conversion of magnesium and sulfur via the formation of a series of intermediate polysulfide MgS_x (2<x<8) has been verified by means of various analytical and electrochemical techniques [43].

The main challenge in Mg battery is the development of an electrolyte for reversible Mg shuttle. The problems are: (1) The need to develop Mg²⁺-ion containing non-aqueous liquid electrolytes with high ionic conductivity and dielectric constant for reversible deposition and dissolution of magnesium. (2) The need to develop a strategy to overcome, or minimize the formation of a passivating layer on the magnesium electrode that might compromise the performance of the rechargeable battery. Carborane based magnesium electrolyte [1-(1,7-carboranyl) magnesium chloride of formula B10C₂ClH₁₁Mg] was found [44] to be electrochemically stable up to ~3.2 V on platinum (for reversible Mg deposition/stripping), stainless steel (316 grade), and aluminum. Bian et al. [45] and Carter [46] also reported the development of thiolate based electrolytes showed an oxidative stability ~2.5 V on platinum electrode with a reversible Mg²⁺-ion insertion/extraction into/from Mo₆S₈

electrode yielding a capacity as high as 40 mA h g⁻¹ when tested at 0.38°C and ~45 mA h g⁻¹ at 0.095°C current rate, respectively.

The discharge performance and the cyclability of the batteries was considerably improved using Non-Nucleophilic Electrolytes such as tetraglyme or a binary solvent of glyme and PP14TFSI, on Mg/S battery [35].

5.4 Sodium ion Battery (SIB)

SIBs have drawn increasing attention for largescale energy storage, because of the natural abundance, low cost and environmental benignity of sodium. SIBs have a theoretical specific capacity of 1165 mAh g⁻¹ with a negative reduction potential of -2.71 V vs. SHE. Since the size of Na⁺ (radius ~1.02 Å) is larger than Li⁺, most materials don't have sufficiently big interstitial space to host Na⁺, leading to sluggish diffusion kinetics of Na⁺ in electrode materials [39]. Therefore, a great challenge for developing SIBs is to find appropriate electrode materials capable of hosting Na⁺ with high capacity and fast diffusion kinetics. For cathode materials, sodium-based transition metal oxides such as carbon modified NaCrO₄ [47] show good electrical property and can accelerate the reversible insertion/extraction of sodium ions and the facile complementary redox reactions of Cr₄₊/Cr₃₊ couple. Na_{1.25}V₃O₈ nanowires as cathode [48] provides an increased electrode– electrolyte contact area, better strain accommodation, prevent self-aggregation and also shorten Na ion diffusion path. Sulfates have been considered as cathode candidates for SIBs Na₂M(SO₄)·4H₂O (M = Mg, Fe, Co or Ni) and their dehydrated derivatives Na₂M(SO₄)₂ (M = Co or Fe) show electrochemical activity at potential 3.3–3.4 V vs. Na/Na [49,50]. For anode materials in SIBs, various carbon materials with different structures [51,52] and different morphologies (such as carbon nanowires and hollow carbon nanospheres) [53,54] have been investigated, normally delivering a reversible capacity of about 250–300 mAh g⁻¹ at a voltage range from 0⁻³ V).

Alloy-based anodes, such as Sn (Na₁₅Sn₄, 847 mAh g⁻¹) and Sb (Na₃Sb, 660 mAh g⁻¹), have attracted considerable interest due to their appropriate potential of Na⁺ insertion and high theoretical capacities for SIBs. Among them, Sn is a promising candidate with an average voltage of 0.3 V (vs. Na/Na⁺) and a theoretical capacity of 790 mAh g⁻¹

Sn nanoparticles homogeneously embedded in spherical carbon network [55] exhibited high electrical conductivity of the Sn/C framework promoting the reversible sodiation/desodiation.

Other batteries in these categories are K ion battery Ca Battery, Al battery, Zn battery which also have high theoretical energy density. But the development of these batteries are rather slow due to problems in finding the right electrode materials.

6. Conclusion

The demand for energy storage device is increasing. New and high energetic inexpensive electrode materials cannot improve the performance of the present existing batteries but also show the route of finding non-Li ion based battery of low cost and high performance. Nano material s metals, alloys, oxides and composite produce very high energetic electrodes materials using abundant materials on earth. Rechargeable batteries base on alternative metal elements (Na, K, Mg, Ca, Zn and Al, etc.)

can provide relatively high-power density and energy density using abundant, low-cost materials. The final choice of anode-cathode couple for a future cell depends on the outcome of various electrochemical testing as described above.

REFERENCES

1. Cheng S, Liu H, Logan BE. Increased power generation in a continuous flow MFC with advective flow through the porous anode and reduced electrode spacing. *Environ Sci Technol.* 2006;40(7):2426-32.
2. Morris JM, Jin S, Wang J, et al. Lead dioxide as an alternative catalyst to platinum in microbial fuel cells. *Electrochem Commun.* 2007;9(7):1730-4.
3. Li Y, Lu A, Ding H, et al. Cr (VI) reduction at rutile-catalyzed cathode in microbial fuel cells. *Electrochem Commun.* 2009;11(7):1496-9.
4. Das D, Sen PK, Das K. Electrodeposited MnO₂ as electrocatalyst for carbohydrate oxidation. *J Appl Electrochem.* 2006;36(6):685-90.
5. Paul S, Ghosh A. Electrochemical characterization of MnO₂ as electrocatalytic energy material for fuel cell electrode. *J Fuel Chem Technol.* 2015;43(03):344-51.
6. Paul S, Chatterjee R. Development of nano carbon-MnO₂ energy material for glucose fuel cell electrode. *Nanomaterials and Energy.* 2015;4(1):64-72.
7. Paul S, Ghosh A. MnO₂, A high electrocatalytic energy material to synthesis energy from oxidation of methanol in fuel cell. *Energy and Environment Focus.* 2015;15:1-7.
8. Guchhait SK, Paul S. Synthesis and characterization of ZnO-Al₂O₃ oxides as energetic electro-catalytic material for glucose fuel cell. *J Fuel Chem Technol.* 2015;43(8):1004-10.
9. Paul S, Naimuddin S, Ghosh A. Electrochemical characterization of Ni-Co and Ni-Co-Fe for oxidation of methyl alcohol fuel with high energetic catalytic surface. *J Fuel Chem Technol.* 2014;42(1):87-95.
10. Paul S, Naimuddin S. Electrochemical characterization of synthesized Ni-Co and Ni-Co-Fe electrodes for methanol fuel cell. *J Fuel Cell Sci Technol.* 2015;12(1):011007.
11. Scibioh MA, Kim SK, Cho EA, et al. Pt-CeO₂/C anode catalyst for direct methanol fuel cells. *Appl Catal B.* 2008;84(3):773-82.
12. Perkins CL, Henderson MA, Peden CH, et al. Self-diffusion in ceria. *J Vac Sci Technol. A: Vacuum, Surfaces, and Films.* 2001;19(4):1942-6.

13. Zhou Y, Gao Y, Liu Y, et al. High efficiency Pt-CeO₂/carbon nanotubes hybrid composite as an anode electrocatalyst for direct methanol fuel cells. *J Power Sources*. 2010;195(6):1605-9.
14. Campos CL, Roldán C, Aponte M, et al. Preparation and methanol oxidation catalysis of Pt-CeO₂ electrode. *J Electroanal Chem*. 2005;581(2):206-15.
15. Paul S. Characterization of bioelectrochemical fuel cell fabricated with agriculture wastes and surface modified electrode materials. *J Fuel Cell Sci Technol*. 2012;9(2):021013.
16. Paul S, Jana A. Study on bio-electrochemical fuel cell with algae. *J Inst Eng Interdiscip*. 2007;504(88):5.
17. Paul S, Mondal P. Pyrolysis of forest residue for production of bio fuel. *Int Energy J*. 2006;7:221-5.
18. Paul S, Mondal P. Fabrication and characterization of bioelectrochemical fuel cell with pyrolysed produced bio oil and hydrolysed biomass by fermentation. *J Inst Eng Interdiscip*. 2009;504(90):5.
19. Hu YS, Kienle L, Guo YG, et al. High lithium electroactivity of nanometer-sized rutile TiO₂. *Advan Mater*. 2006;18(11):1421-6.
20. Sorensen EM, Barry SJ, Jung HK, et al. Three-dimensionally ordered macroporous Li₄Ti₅O₁₂: effect of wall structure on electrochemical properties. *Chem Mater*. 2006;18(2):482-9.
21. Zhong K, Xia X, Zhang B, et al. MnO powder as anode active materials for lithium ion batteries. *J Power Sources*. 2010;195(10):3300-8.
22. Gao J, Lowe MA, Abruna HD. Spongelike nanosized Mn₃O₄ as a high-capacity anode material for rechargeable lithium batteries. *Chem Mater*. 2011;23(13):3223-7.
23. Qiu Y, Xu GL, Yan K, et al. Morphology-conserved transformation: synthesis of hierarchical mesoporous nanostructures of Mn₂O₃ and the nanostructural effects on Li-ion insertion/deinsertion properties. *J Mater Chem*. 2011;21(17):6346-53.
24. Reddy AL, Shaijumon MM, Gowda SR, et al. Coaxial MnO₂/carbon nanotube array electrodes for high-performance lithium batteries. *Nano Lett*. 2009;9(3):1002-6.
25. Zhang WM, Wu XL, Hu JS, et al. Carbon Coated Fe₃O₄ Nanospindles as a Superior Anode Material for Lithium-Ion Batteries. *Adv Funct Mater*. 2008;18(24):3941-6.
26. Reddy MV, Yu T, Sow CH, et al. α-Fe₂O₃ nanoflakes as an anode material for Li-ion batteries. *Adv Funct Mater*. 2007;17(15):2792-9.
27. Kang YM, Song MS, Kim JH, et al. A study on the charge–discharge mechanism of Co₃O₄ as an anode for the Li ion secondary battery. *Electrochimica Acta*. 2005;50(18):3667-73.

28. Liu H, Wang G, Liu J, et al. Highly ordered mesoporous NiO anode material for lithium ion batteries with an excellent electrochemical performance. *J Mater Chem*. 2011;21(9):3046-52.
29. Lou XW, Wang Y, Yuan C, et al. Template-free synthesis of SnO₂ hollow nanostructures with high lithium storage capacity. *Adv Mater*. 2006 Sep 5;18(17):2325-9.
30. Chen JS, Lou XW. SnO₂-based nanomaterials: Synthesis and application in lithium-ion batteries. *small*. 2013;9(11):1877-93.
31. Courtney IA, Dahn JR. Electrochemical and *in situ* X-ray diffraction studies of the reaction of lithium with tin oxide composites. *J Electrochem Soc*. 1997;144(6):2045-52.
32. Zhou X, Wan LJ, Guo YG. Binding SnO₂ nanocrystals in nitrogen-doped graphene sheets as anode materials for lithium-ion batteries. *Adv Mater*. 2013;25(15):2152-7.
33. Wang X, Cao X, Bourgeois L, et al. N-doped graphene-SnO₂ sandwich paper for high-performance lithium-ion batteries. *Adv Funct Mater*. 2012;22(13):2682-90.
34. Paek SM, Yoo E, Honma I. Enhanced cyclic performance and lithium storage capacity of SnO₂/graphene nanoporous electrodes with three-dimensionally delaminated flexible structure. *Nano Lett*. 2008;9(1):72-5.
35. Zhang HX, Feng C, Zhai YC, et al. Cross-stacked carbon nanotube sheets uniformly loaded with SnO₂ nanoparticles: A novel binder-free and high-capacity anode material for lithium-ion batteries. *Adv Mater*. 2009;21(22):2299-304.
36. Reddy MA, Fichtner M. Batteries based on fluoride shuttle. *J Mater Chem*. 2011;21(43):17059-62.
37. Rongeat C, Anji-Reddy M, Witter R, et al. Solid electrolytes for fluoride ion batteries: ionic conductivity in polycrystalline tysonite-type fluorides. *Appl Mater Interfaces*. 2014;6(3):2103-10.
38. Rongeat C, Reddy MA, Diemant T, et al. Development of new anode composite materials for fluoride ion batteries. *J Mater Chem A*. 2014;2(48):20861-72.
39. Zhao-Karger ZH, Zhao X, Fuhr O, et al. Bisamide based non-nucleophilic electrolytes for rechargeable magnesium batteries. *RSC Adv*. 2013;3(37):16330.
40. Murin IV, Glumov OV, Mel'nikova NA. Solid electrolytes with predominant chloride conductivity. *Russ J Electrochem*. 2009;45(4):411-6.
41. Stevens DA, Dahn JR. The mechanisms of lithium and sodium insertion in carbon materials. *J Electrochem Soc*. 2001;148(8):A803-11.

42. Wang YX, Chou SL, Liu HK, et al. Reduced graphene oxide with superior cycling stability and rate capability for sodium storage. *Carbon*. 2013;57:202-8.
43. Imanaka N, Okamoto K, Adachi G. Water-insoluble lanthanum oxychloride-based solid electrolytes with ultra-high chloride ion conductivity. *Angew Chem Int Ed*. 2002;41(20):3890–2.
44. Yamada K, Kuranaga Y, Ueda K, et al. Phase transition and electric conductivity of ASnCl_3 (A = Cs and CH_3NH_3). *Bull Chem Soc Jpn*. 1998;71(1):127-34.
45. Zhao-Karger Z, Zhao X, Wang D, et al. Performance Improvement of Magnesium Sulfur Batteries with Modified Non-Nucleophilic Electrolytes. *Adv Energy Mater*. 2015;5(3).
46. Carter TJ, Mohtadi R, Arthur TS, et al. Boron clusters as highly stable magnesium-battery electrolytes. *Angew Chem Int Ed*. 2014;53(12):3173-7.
47. Bian P, NuLi Y, Abudoureyimu Z, et al. A novel thiolate-based electrolyte system for rechargeable magnesium batteries. *Electrochim Acta*. 2014;121:258-63.
48. Bian PW, Nuli YN, Yang J, et al. Benzenethiolate-based solutions for rechargeable magnesium battery electrolytes. *Acta Phys Chim Sin*. 2014;30(2):311-7.
49. Yu CY, Park JS, Jung HG, et al. NaCrO_2 cathode for high-rate sodium-ion batteries. *Energy Environ Sci*. 2015;8(7):2019-26.
50. Dong Y, Li S, Zhao K, et al. Hierarchical zigzag $\text{Na}_1.25\text{V}_3\text{O}_8$ nanowires with topotactically encoded superior performance for sodium-ion battery cathodes. *Energy Environ Sci*. 2015;8(4):1267-75.
51. Reynaud M, Rousse G, Abakumov AM, et al. Design of new electrode materials for Li-ion and Na-ion batteries from the bloedite mineral $\text{Na}_2\text{Mg}(\text{SO}_4)_2 \cdot 4\text{H}_2\text{O}$. *J Mater Chem A*. 2014;2(8):2671-80.
52. Barpanda P, Oyama G, Ling CD, et al. Kröhnkite-type $\text{Na}_2\text{Fe}(\text{SO}_4)_2 \cdot 2\text{H}_2\text{O}$ as a novel 3.25 V insertion compound for Na-ion batteries. *Chem Mater*. 2014;26(3):1297-9.
53. Cao Y, Xiao L, Sushko ML, et al. Sodium ion insertion in hollow carbon nanowires for battery applications. *Nano Letters*. 2012;12(7):3783-7.
54. Tang K, Fu L, White RJ, et al. Hollow carbon nanospheres with superior rate capability for sodium-based batteries. *Adv Energy Mater*. 2012;2(7):873-7.
55. Xu Y, Zhu Y, Liu Y, et al. Electrochemical performance of porous carbon/tin composite anodes for sodium-ion and lithium-ion batteries. *Adv Energy Mater*. 2013;3(1):128-33.